7N-02
194261
43P.

TECHNICAL NOTE
D-35

FULL-SCALE WIND-TUNNEL INVESTIGATION OF THE LONGITUDINAL CHARACTERISTICS OF A TILTING-ROTOR CONVERTIPLANE

By David G. Koenig, Richard K. Greif,
and Mark W. Kelly

Ames Research Center
Moffett Field, Calif.

NATIONAL AERONAUTICS AND SPACE ADMINISTRATION

WASHINGTON December 1959

(NASA-TN-D-35) FULL-SCALE WIND-TUNNEL INVESTIGATION OF THE LONGITUDINAL CHARACTERISTICS OF A TILTING-ROTOR CONVERTIPLANE (NASA. Ames Research Center) 43 p

N89-70796

Unclas
00/02 0194261

NATIONAL AERONAUTICS AND SPACE ADMINISTRATION

TECHNICAL NOTE D-35

FULL-SCALE WIND-TUNNEL INVESTIGATION OF THE LONGITUDINAL CHARACTERISTICS OF A TILTING-ROTOR CONVERTIPLANE

By David G. Koenig, Richard K. Greif,
and Mark W. Kelly

SUMMARY

Tests of a tilting-rotor convertiplane, currently designated the XV-3, were made to investigate both mechanical and aerodynamic aspects of this type of aircraft. Only the longitudinal aerodynamic characteristics are the subject of this report.

Aircraft configuration variables were angle of attack, rotor-pylon angle, power, and longitudinal control. With the exceptions of a few runs at or near zero airspeed, and several propulsive efficiency runs at airspeeds up to 155 knots, most of the tests were made between approximately 60 and 120 knots. The tests at a given airspeed and pylon angle usually consisted in varying one of the aircraft variables with the others held constant. For each pylon angle setting, trim control and power settings simulating level flight of 4700 pounds gross weight were experimentally determined for at least one airspeed.

The XV-3 rotor was found to perform well aerodynamically, both as a helicopter rotor and as a propeller for the present XV-3 configuration. Although reducing rotor speed might increase somewhat the operating propulsive efficiency of the XV-3, large rotor flapping angles resulting at low rotor speeds will probably serve as a lower limit to rotor speed. The XV-3 was found longitudinally stable with the moment center near the pivot line of the pylon for pylon angles between about 10° and 90° at airspeeds above 60 knots. Several steady-state conversion processes were defined and the choice of any one does not seem to depend on the speed-power requirements.

INTRODUCTION

Several methods of vertical take-off and landing are currently being studied. One of the methods is that of tilting rotors which enable the aircraft to take off and land in a helicopter configuration while, for airplane flight, the rotors are tilted forward to serve as propellers.

This method is represented currently by a full-scale aircraft designated the Bell XV-3 on which helicopter-type rotors are pylon mounted at each wing tip. Conversion from helicopter to airplane flight theoretically is possible in several ways. Lift can be transferred to the wing gradually by increasing speed at a high angle of attack; alternately, lift can be kept on the rotors until a speed is reached where the wing can support the aircraft completely with the conversion being made at nearly constant airspeed. Many combinations of these extremes may be possible and flight experience alone will establish the most desirable procedure.

Initial flights of the XV-3 revealed a wing-pylon rotor oscillation existing at high forward speed and partial rotor lift which prevented successful conversion. The subject wind-tunnel studies of the prototype XV-3 were made, therefore, to study the effectiveness of a number of modifications designed to eliminate this oscillation. These studies were of value in the respect that sufficient information was obtained to enable continuation of the flight test program. In the course of the specific structural and mechanical study in the wind tunnel, a considerable amount of aerodynamic data were obtained concerning the static longitudinal characteristics of the convertiplane.

The purpose of the present report is to present these aerodynamic data and to interpret them to the extent possible in terms of performance and stability and control of the XV-3.

NOTATION

The angle convention used herein is shown in figure 1.

b wing span, ft

c_r rotor chord, ft

c_w wing chord, ft

$\bar{c}_t$ mean aerodynamic chord of the horizontal tail

C_D drag coefficient, $\frac{\text{drag}}{qS_w}$

C_{D_r} drag coefficient due to rotor, $\frac{\text{rotor drag}}{qS_w}$

C_{D_w} drag coefficient obtained with rotor blades off

C_L lift coefficient, $\frac{\text{lift}}{qS_w}$

C_{L_r}	lift coefficient due to the rotor, $\frac{\text{rotor lift}}{qS_W}$
C_{L_W}	lift coefficient obtained with rotor blades off
C_m	pitching-moment coefficient, $\frac{\text{moment}}{qS_Wc_W}$
C_P	power coefficient per rotor, $\frac{550P_r}{2\rho n^3D^5}$
C_T	thrust coefficient per rotor, $\frac{2T}{\pi^3\rho n^2D^4}$
D	rotor diameter, ft
J	$\frac{V_\infty}{nD}$
l_t	distance from 28-percent wing chord (moment center position) to $\frac{\bar{c}_t}{4}$, ft
l_p	distance from pylon pivot to teetering hinge of the rotor, ft
M	figure of merit, $\frac{1.414R}{550P_r}\sqrt{\frac{R}{\rho\pi D^2}}$
n	rotor speed, rps
P_r	total power supplied to both rotors measured at rotor pylons, hp
q	dynamic pressure, lb/sq ft
R	total resultant force acting on the aircraft, lb
S_r	total rotor area, $2\left(\frac{\pi D^2}{4}\right)$, sq ft
S_t	area of horizontal tail, sq ft
S_W	total wing area extending from aircraft plane of symmetry to outer edge of the tip fairing, sq ft
T	total rotor thrust, or propulsive thrust, lb
V_∞	free-stream velocity, knots or ft/sec
α	angle of attack of the fuselage reference line (see fig. 2), deg

α_p pylon angle, angle of pylon forward from perpendicular to fuselage reference line, deg

α_r rotor angle of attack with reference to control axis, negative when control axis is tilted forward, deg

β rotor flapping measured in a plane parallel with free stream with reference to the control axis, deg

γ angle between the resultant rotor force vector and the control axis, positive when rotor force vector is tilting downstream, deg

δ elevator deflection, positive with trailing edge down, deg

η propulsive efficiency, $\frac{TV_\infty}{550P_r}$

θ cyclic pitch, angle between the forward displacement of the control axis (normal to the plane of no flapping) and the pylon, deg

σ rotor solidity, $\frac{2Bc_r}{\pi D}$ where B is the number of blades and c_r is blade chord

φ angle between the pylon and a line intersecting the moment center and flapping axis as measured in plane parallel to the plane of symmetry, deg

AIRPLANE AND TEST EQUIPMENT

Photographs of the XV-3 convertiplane mounted in the Ames 40- by 80-foot wind tunnel are presented in figures 2(a) and (b). One of the rotor head assemblies is shown in figure 2(c). A three-view sketch of the aircraft is shown in figure 3, and pertinent geometric data are listed in table I.

The XV-3 convertiplane consists basically of a conventional airplane design combined with pylon-mounted helicopter-type rotors at the wing tips. The pylons are free to tilt through a 90° angular range bracketed by the helicopter pylon position at $\alpha_p = 0^\circ$ and the airplane pylon position at $\alpha_p = 90^\circ$. Power was supplied through center and wing-tip transmissions by a reciprocating aircraft-type engine of 450-horsepower-rated power output. Two rotor-to-engine speed ratios were possible; the higher rotor speeds chosen principally for helicopter and conversion flight conditions, and the lower speed chosen for airplane flight conditions.

Longitudinal control in hovering and conversion flight was obtained on the aircraft by cyclic pitch change on the rotors coupled with elevator deflection. The mechanical linkage between the elevator and control stick was the same for all pylon positions. At 0° pylon angle, control stick movement altered both cyclic pitch and elevator deflection in a ratio that gave a 4° change in elevator deflection for a 1° change in cyclic pitch. The ratio of cyclic pitch change to stick movement decreased linearly with pylon angle to reach zero as the pylon angle reached 90°.

The collective pitch was controlled through a separate pitch control stick. The collective pitch was linked mechanically to pylon movements so that for any given pitch control setting, the actual blade collective pitch increased linearly with pylon angle. The collective pitch increase for a pylon movement from 0° to 90° was 12°. Lateral and directional control were achieved by means of differential collective and cyclic pitch, coupled with aileron and rudder movements.

All flight controls, including engine controls, collective pitch, and main control sticks, were controlled remotely from a console located outside the tunnel test section. Control settings were indicated directly on the console instrument panel.

TESTS AND PROCEDURE

All tests considered herein were made with the short pylon.

Because the primary purpose of the test was a structural-mechanical study, it was necessary to approximate true flight conditions as far as loads (lift of 4700 pounds and zero drag) and airspeed were concerned. In the interest of obtaining useful aerodynamic information, an attempt was made to approach longitudinal trim through adjustment of power, cyclic pitch, and elevator deflection. Finally, to aid in the analysis, the variations of airplane characteristics with angle of attack, power, and longitudinal control were determined for most of the established trim conditions.

For the conversion study, the test procedure was such that flight conditions were approximately established for one airspeed at $\alpha_p = 10^\circ$ (V_∞ = 80 knots), 30° (V_∞ = 80 knots), 60° (V_∞ = 100 knots), and 90° (V_∞ = 100 knots) with a rotor speed of 532 rpm. At each pylon angle data were obtained at these conditions and one or two other airspeeds for the same control and power settings (with the exception of $\alpha_p = 90^\circ$). Other tests were made near $V_\infty = 0$ in the helicopter configuration for $\alpha_p = 5^\circ$ and a rotor speed of 532 rpm and at airspeeds between 80 and 155 knots in the airplane configuration for $\alpha_p = 90^\circ$ with rotor speeds between 250 and 300 rpm. The angle-of-attack range for the tests was from about -4° to $+14^\circ$. Longitudinal control range was from -12° to $+12^\circ$ of elevator. The range of each of the variables was limited occasionally by structural or dynamic considerations, such as 5200 pounds lift or 9° blade flapping. Longitudinal data were also obtained with the blades removed.

The moment center was located near the 28-percent wing-chord line.

CORRECTIONS TO DATA

No wind-tunnel wall corrections have been applied to the data used in the present report. For an estimation of these effects, the reader is referred to reference 1 where a method is outlined for computing these effects for the XV-3 type aircraft. With this procedure, the corrections are found to be

$$\Delta\alpha = a_{\alpha} + 0.26C_{L_w} + 0.27\sqrt{C_{L_r}C_{L_w}} + 0.26C_{L_r}$$

where a_{α} is a constant in the order of 0.05, and C_{L_r} may be approximated by subtracting rotor-blades-off lift, C_{L_w}, from total lift.

$$\Delta C_D = \frac{\Delta\alpha}{57.5} C_L$$

$$\Delta C_m = 0.011C_{L_w} + 0.003\left(\frac{l_t}{c_w}\right)_r C_{L_r} + 0.011\sqrt{C_{L_r}C_{L_w}}$$

where

$$\left(\frac{l_t}{c_w}\right)_r = 3.64 + \frac{l_p}{c_w}\sin\alpha_p \qquad .$$

Although taken into account in the derivation of trim conditions, strut drag and moment tares were not applied to the basic data. Tares were estimated by measuring drag on the strut alone with fuel line and instrumentation leads simulated. The pitching-moment strut tare was found negligible, and drag tare based on wing area of the aircraft was found to be $C_{D_{tare}} = 0.022$.

RESULTS AND DISCUSSION

Performance

A tilting-rotor-type VTOL aircraft presents the problems of designing a rotor to give good performance in both hovering and forward flight. A brief study was made of the XV-3 rotor in hovering and airplane flight conditions to determine how its design met these widely differing requirements. Since it was impossible to measure rotor thrust and rotor power of one isolated rotor, the results include some interference effects.

Hovering performance.- Resultant force as a function of rotor power was measured at approximately zero forward speed with the fuselage at 0° angle. The top of the wind-tunnel test section was open and the pylon was set at $\alpha_p = 5^{\circ}$ in order to minimize circulation; since the rotor pylons were about 24 feet from the floor, it is probable that the ground effect was negligible. The resulting measurements are shown in figure 4(a), and figure 4(b) shows the figure of merit as calculated from the resultant force and the corresponding rotor power. Also shown in figure 4(b) is the figure of merit calculated by the method of reference 2 (eq. 8, pp. 51 and 72). The failure of the XV-3 rotor to realize the calculated figure of merit can be explained in part by the download on the wing which is included in the resultant force measurements. An estimate of this download based on flat plate drag and uniform rotor downwash indicates that it would account for close to one-half the difference between measured and theoretical figure of merit for $R = 3000$ pounds. It is also possible that recirculation of the rotor slipstream in the wind-tunnel test section accounted for part of the difference between the experimental and calculated figure of merit, although, as mentioned above, an effort was made to minimize this effect. These results indicate that the rotor approached the figure of merit of good helicopter rotors which exhibit the highest hovering performance of most current VTOL designs.

Rotor forward flight performance.- Propulsive thrust, $-(C_{D_r})_{\alpha=0}$, and power variations were obtained for a range of J values typical of airplane flight within limits imposed by power and collective pitch. The results of this study are shown in figure 5 in terms of the variation of η with J for constant values of C_p.

It is evident that if proper combinations of J and C_p can be realized in cruising flight, the rotor will operate as a propeller with efficiencies of over 80 percent. Calculations were made to determine the rotor efficiency when operating as a propeller under cruise conditions of the XV-3. Drag measurements of the XV-3 show that at rated engine horsepower ($P_r = 362$ hp which for a rotor speed of 275 rpm would be equivalent to $C_p = 0.07$), the XV-3 would attain a forward flight speed of 125 knots; the rotor would be operating at a propulsive efficiency of about 78 percent (fig. 5). The propulsive efficiency is reasonably high at this combination of speed, power ($C_p = 0.07$), and rotor rpm (275); however, speed increases resulting from drag reduction could be expected since the drag of the experimental machine seems high ($C_{D_{min}} = 0.1$ with strut tares removed). From figure 5 it can be seen that any speed increase at constant rpm and C_p will result in a rapid drop in efficiency; in addition, it may be shown from the data of figure 5 that a reduction in rpm at constant air speed for level flight of the XV-3 should result in an increase in efficiency. Measurements of blade flapping have shown, however, that this characteristic may place a definite limit on the extent to which rotor speed can be reduced. Blade flapping angles measured for values of rotor power and speed typical of those used for conversion and helicopter flight are presented in figure 6(a). It is evident from the data that flapping angles would probably not exceed 5° in helicopter flight ($\alpha_p = 10^\circ$) and about 2° in airplane flight ($\alpha_p = 90^\circ$) for this rotational speed range. Flapping measurements which are presented in figure 6(b) for the lower rotor speed (275 rpm) proposed for use in airplane cruising flight show, however, that lower rotor speed has increased the flapping angles and there is evidenced a rapid increase in flapping angle with wing angle of attack. The fact that higher flight speeds result in lower angles of attack, for equal lift, compensates to some degree for the increased flapping. It is possible that this flapping could be controlled by mechanical changes to the XV-3 rotor-pylon system, such as increasing the value of pitch flap coupling (present value was approximately -0.36 blade pitch change per degree flapping) or increasing the pylon angle to some value greater than 90° for trimmed level airplane flight.

The foregoing results seem to show the significance of the compromise required in the choice of a rotor design for an XV-3 type aircraft. In the case of the XV-3 in airplane flight, rotor characteristics are well matched to the drag characteristics of the airplane configuration tested. However, drag reductions are possible in future designs. If the drag coefficient is reduced, and the rotor is operated at the same advance ratio, the rotor C_p must likewise be reduced, leading to a loss in propulsive efficiency. If rotor diameter or solidity is reduced to alleviate this loss in efficiency, a reduction in hovering performance will probably result. On the other hand, if the rotor is operated at higher advance ratios and power coefficients to alleviate this loss in efficiency, the blade flapping problem would probably be accentuated.

Longitudinal Stability and Control

The longitudinal characteristics of the XV-3 were used to predict some of the conversion and airplane flight characteristics of the machine. Because of limitations in test capabilities, no consideration is made of the hovering or very low-speed helicopter flight cases. For these cases, however, the XV-3 should exhibit characteristics similar to a conventional single rotor helicopter insofar as longitudinal stability and control are concerned.

2K

A-165

Basic force and moment data. - Basic force and moment data obtained at varying angle of attack are presented in figure 7 for the aircraft with rotor blades off and in figure 8 for the aircraft with the rotor blades on. As was mentioned, the rotor-on data were obtained at constant power; rotor speed was held constant for a given airspeed or pylon angle by changing collective pitch.

Although a large amount of the power-on data were obtained for control and power settings somewhat off those of trimmed level flight, two conclusions may be drawn from the data of figure 8. As evidenced from comparisons of the basic pitching-moment data, the XV-3 is statically stable (with the moment center location at 28-percent chord) for all conditions but this stability generally decreases with reduced pylon angle and airspeed (for lift coefficients near those required for level flight at 4700 pounds lift). This is probably a consequence of the destabilizing influence of the rotors as helicopter flight is approached and as the stabilizing influence of the horizontal tail decreases with decreasing airspeed. A second important indication of the basic data is evidenced in the breaks of the curves of figure 8(b) for $\alpha_p = 30^\circ$ which are believed to be the result of wing stall. Since it might be undesirable to start conversion below the wing stalling speed, the use of wing flaps or some other high-lift device for reducing the minimum airspeed for conversion is worthy of consideration.

In addition to the data of figures 7 and 8, data were also obtained to determine the effect of varying power or longitudinal control through a short range at a constant angle of attack. These data, presented in table II in terms of the derivatives, were used to obtain trim conditions, as will be discussed subsequently.

The longitudinal control effectiveness (C_{m_θ}) measured under several conditions is presented in table II. For one condition where cyclic pitch was expected to contribute significantly to C_{m_θ} ($\alpha_p = 10^\circ$) the variation of C_m with θ for constant collective pitch and rotor speed was determined, first with the normal elevator variation and then with the elevators locked at 0°. These results are presented in figure 9 and show that the rotor contributed little to C_{m_θ}. Since collective pitch and rotor speed were held constant for these tests, some reduction in thrust (about 16 percent) resulted as cyclic pitch was changed. It might be anticipated that the value of C_{m_θ} obtained for conditions of constant thrust would differ from that obtained for constant collective pitch and rotor speed, and calculated results showing the order of this difference are also presented in figure 9. (These calculations were made using values of thrust derived from the charts of reference 3, and assuming that the thrust acted in a direction parallel to the rotor control axis.) The calculated results indicate that C_{m_θ} would be increased by holding rotor thrust constant rather than collective pitch or rotor speed. However, for either case, the contribution of the rotor to C_{m_θ} is much smaller than that of the elevators. Also, the experimental C_{m_θ} is less than the computed C_{m_θ}, and it is believed that interference effects of the rotor slipstream on the flow around the airplane may be responsible for the difference. The possibility of these interference effects is supported by consideration of the rotor contribution to C_m. As shown in figure 9, the rotor contributed a large nose-down increment to C_m. However, if the rotor contributions to C_L and C_D are multiplied by their respective moment arms, a significant nose-up moment is obtained.

Control and power settings for trimmed level flight.- As has been mentioned (see Tests and Procedure), control and power settings for trimmed level flight were established during the tests for one airspeed per pylon angle setting and were not changed for tests made at other airspeeds. In order to establish the variation of trim power and control settings with airspeed, the out-of-trim data for these other airspeeds were adjusted with the aid of the derivatives given in table II. The procedure used in these computations is described in the appendix.

The accuracy of this process depends, of course, to a large extent on the accuracy with which the derivatives can be determined. Those of most significance proved to be the ones which were well defined by experiment, and those which were not determined experimentally but were estimated by calculation were found to have little effect on the adjusting process.

The variation with airspeed of rotor power, stick position (elevator setting), and angle of attack required for trim for four pylon angles are presented in figures 10(a), (b), and (c), respectively. Since trim data at only two or three airspeeds for each pylon angle could be estimated from the data, the fairing of the power curves of figure 10(a) was somewhat arbitrary; these curves were faired under the assumption that an envelope to the curves existed which represented a conversion process of minimum power. The data of figure 10 were used to define conversion processes described in the following section.

Conversion processes.- From the variation of trim conditions shown in figure 10, it is possible to estimate some of the characteristics of the XV-3 during conversion. With the freedom available in the distribution of lift between the wing and rotor, an infinite number of conversion schedules are possible. Only four of them are considered here; they are conversion at a constant airspeed and conversion at variable airspeed either at minimum power or with two stick-fixed positions. Without flight experience, it is not possible to judge which schedule will satisfy pilot requirements. Acceleration effects are not considered in the study.

A level flight conversion process at a constant airspeed of 100 knots is described by the data of figure 11. To fully describe conversion at this speed, it was necessary to assume a slightly higher maximum lift on the wing than was possible on the actual aircraft (with stalling speed in airplane configuration of about 103 knots). If the pylon angle were increased continuously for this type of conversion, altitude at constant airspeed could be maintained by a continuous movement of control stick coordinated with an adjustment of power. If mechanical or dynamic requirements dictate a near-constant rotor speed during the process, as was the case for the XV-3, the collective pitch as coordinated with the throttle would have to be adjusted continually for a continuous conversion. In the case of the subject aircraft, this adjustment is augmented by the mechanical linkage between collective pitch and pylon angle.

Three conversion processes at varying airspeeds are presented in figure 12. Conversion at minimum required power is defined by the envelope to the curves of figure 10(a). Values of required elevator setting presented in the figure corresponding to this process indicate that stick movement is stable with speed for pylon angles below 30° and approximately neutrally stable for higher pylon angles. The remaining two processes shown in figure 12 are for longitudinal control with the stick fixed for two different stick positions. It may be seen that the speed and power requirements for these processes do not vary appreciably from that of the minimum power process. From this it appears that the choice among several possible conversion processes will be determined by factors other than the speed and power requirements.

CONCLUDING REMARKS

Rotor Characteristics

Although the hovering performance of the XV-3 rotor is similar to that required of a helicopter rotor, the operating propulsive efficiency at the design rotor speed proposed for airplane flight is high, being close to 80 percent. Even though lower rotor speed might increase propulsive efficiency somewhat above this value, the occurrence of large flapping angles at low rotor speeds will probably serve as a lower limit to rotor speed.

Longitudinal Stability and Control

With the moment center located just below the pylon pivot line, the XV-3 is longitudinally stable for airspeeds above 60 knots and for pylon angles between 10° and 90°. However, large changes in the neutral point location occur with changes in pylon angle and airspeed.

The elevator is the principal source of control for airspeeds of 60 knots and above even though cyclic pitch change is linked with elevator movement at lower pylon angles.

Conversion Processes

A brief analysis has shown that there are several different ways of converting from helicopter forward flight to airplane flight. Several processes differing in the variation of pylon angle with airspeed have approximately the same variation of power with airspeed, this variation being close to the minimum power variation.

Ames Research Center
National Aeronautics and Space Administration
Moffett Field, Calif., May 4, 1959

APPENDIX

DERIVATION OF TRIM CHARACTERISTICS

Control and power adjustments, $\Delta\alpha$, $\Delta\theta$, and ΔP_r, required to change lift, drag, and pitching moment by given values of ΔC_L, ΔC_D, and ΔC_m from that of the test conditions to that of trimmed level flight were obtained by solving the following three equations.

$$\frac{dC_L}{d\alpha}\Delta\alpha + \frac{dC_L}{d\theta}\Delta\theta + \frac{dC_L}{dP_r}\Delta P_r = \Delta C_L$$

$$\frac{dC_D}{d\alpha}\Delta\alpha + \frac{dC_D}{d\theta}\Delta\theta + \frac{dC_D}{dP_r}\Delta P_r = \Delta C_D$$

$$\frac{dC_m}{d\alpha}\Delta\alpha + \frac{dC_m}{d\theta}\Delta\theta + \frac{dC_m}{dP_r}\Delta P_r = \Delta C_m$$

In this analysis, it was assumed that ΔC_L, ΔC_D, and ΔC_m were small enough so that the derivatives $dC_L/d\alpha$, $dC_L/d\theta$ . . . could be regarded as constants. The values of ΔC_L, ΔC_D, and ΔC_m used to attain trimmed level flight conditions are indicated by the leaders of figure 7.

Values of the derivatives used are presented in table II. Data from which the derivatives describing longitudinal control and power effects were evaluated are not presented herein, but it should be mentioned that the derivatives were usually measured at or near the trim lift coefficient. The limitation on range in test variables restricted the number of derivatives which could actually be measured from test data.

The derivatives not obtained for all airspeeds were dC_L/dP_r, dC_D/dP_r, and dC_m/dP_r, but values of these derivatives were measured for airspeeds at which the aircraft was actually trimmed during the test (i.e., an intermediate speed). For other airspeeds, these values, with the exception of dC_m/dP_r were corrected using relations derived as follows. It will be assumed that

$$C_{D_r} = - kC_T \sin(\gamma + \alpha_r)$$

and

$$C_{L_r} = kC_T \cos(\gamma + \alpha_r)$$

represent the rotor contribution to drag and lift of the aircraft. Next, it will be necessary to assume that effects of rotor downwash on the wing are negligible when the lift and drag contribution of the rotor is considered. Then, if C_{D_r} and C_{L_r} are differentiated with respect to P_r they become, respectively,

$$\frac{dC_D}{dP_r} = -\left[k \frac{dC_T}{dP_r} \sin(\gamma + \alpha_r) + kC_T \frac{d\gamma}{dP_r} \cos(\gamma + \alpha_r)\right]$$

$$\frac{dC_L}{dP_r} = k \frac{dC_T}{dP_r} \cos(\gamma + \alpha_r) - kC_T \frac{d\gamma}{dP_r} \sin(\gamma + \alpha_r)$$

where

$$k = 2 \frac{S_r}{S_W} \frac{(nD)^2}{V_\infty^{\,2}}$$

A few numerical examples have shown that the second terms could be neglected while maintaining accuracy consistent with the consequence of neglecting any possible rotor-wing fuselage-tail interference effects. The extrapolation was then made with the proportionalities,

$$\frac{dC_D}{dP_r} \sim \frac{dC_T}{dP_r} \frac{\sin(\gamma + \alpha_r)}{V_\infty^{\,2}}$$

and

$$\frac{dC_L}{dP_r} \sim \frac{dC_T}{dP_r} \frac{1}{V_\infty^{\,2}}$$

on the assumption that

$$\cos(\gamma + \alpha_r) = \text{constant} \approx 1 \qquad (\text{for } \alpha_p = 10^\circ \text{ and } 30^\circ)$$

Since it was evident that the value of dC_m/dP_r was less affected by the rotor contribution than by the effect of the rotor wake on the tail, the measured value of this derivative was used for all speeds.

Values of dC_T/dP_r were obtained using the rotor performance charts of reference 3. The values of γ were obtained from the test data for corresponding airspeeds. In order to obtain α_r and hence dC_L/dP_r or dC_D/dP_r, it was first necessary to assume a value of $\Delta\alpha_r = \Delta\alpha$. Control adjustments were then computed with the use of initial values of dC_L/dP_r and dC_D/dP_r. The new value of $\Delta\alpha = \Delta\alpha_r$ was then used to repeat the calculation. Since the control adjustment, $\Delta\alpha$, was insensitive to changes in dC_L/dP_r and dC_D/dP_r only one recalculation of $\Delta\alpha$ was necessary.

REFERENCES

1. Vaughan, J.: Wind-Tunnel Investigation of the Conversion Process of the Bell Model 200 Convertiplane Model. Vol. I. Analysis and Discussion of Results. Rep. 200-094-229, Bell Helicopter Corp., Aug. 4, 1953.

2. Gessow, Alfred, and Myers, Garry C., Jr.: Aerodynamics of the Helicopter. The Macmillan Co., 1952.

3. Tapscott, Robert J., and Gessow, Alfred: Supplementary Charts for Estimating Performance of High-Performance Helicopters. NACA Rep. 1266, 1956. (Supersedes NACA TN 3482)

A-165

TABLE I.- GEOMETRIC DATA

Wing	
Area (including wing-tip fairing), sq ft	116.0
Span (distance between rotor pylons), ft	29.5
Aspect ratio (based on distance between pylons)	7.5
Incidence, deg	5
Airfoil section	NACA 23021
Fuselage	
Length, ft	30.33
Depth	5.31
Maximum width, ft	4.05
Horizontal tail	
S_t/S_w	0.281
l_t/c	3.64
Elevator area, sq ft	13.9
Rotor	
Diameter (unless otherwise noted), ft	23.00
Blade section	NACA 0015
Chord, in	11.0
Solidity, σ	0.0507
Blade twist, deg/ft radius	-1.60
Power plant	
USAF designation	R-985-AN-1
Normal ratings (hp/rpm/alt)	450/2300/2300
Transmission gear ratios (over-all engine to rotor ratio)	
High rotor speed	4.320:1
Low rotor speed	8.64:1

A-165

TABLE II.- STABILITY PARAMETERS USED IN DERIVING TRIM CHARACTERISTICS

Pylon angle, α_p	10°			30°		60°		90°	
Airspeed, knots	60	80	100	80	100	100	110	100	120
$\frac{dC_L}{d\alpha}$	0.240	0.194	0.152	0.122	0.099	0.094	0.094	0.083	0.089
$\frac{dC_D}{d\alpha}$	.043	.024	.016	.014	.011	.010	.007	.011	.007
$\frac{dC_m}{d\alpha}$	-.060	-.050	-.041	-.041	-.035	-.034	-.034	-.032	-.030
$\frac{dC_L}{d\theta}$	-.122	-.080	-.051	.008	.008	.035	.029	.036	.036
$\frac{dC_D}{d\theta}$	-.056	-.024	-.015	-.003	0	.003	.002	.001	.001
$\frac{dC_m}{d\theta}$	-.20	-.17	-.16	-.16	-.16	-.15	-.15	-.13	-.13
$\frac{dC_L}{dP_r}$	[1].0104	.0079	[1].0054	[1].0046	.0034	.0012	.0013	.0003	.0003
$\frac{dC_D}{dP_r}$	[1]-.0003	-.0003	[1]-.0003	[1]-.0013	-.0011	-.0008	-.0008	-.0012	-.0007
$\frac{dC_m}{dP_r}$	[1]-.0018	-.0018	[1]-.0018	[1]0	0	0	0	0	.0006

[1]Values estimated from helicopter rotor theory (ref. 3).

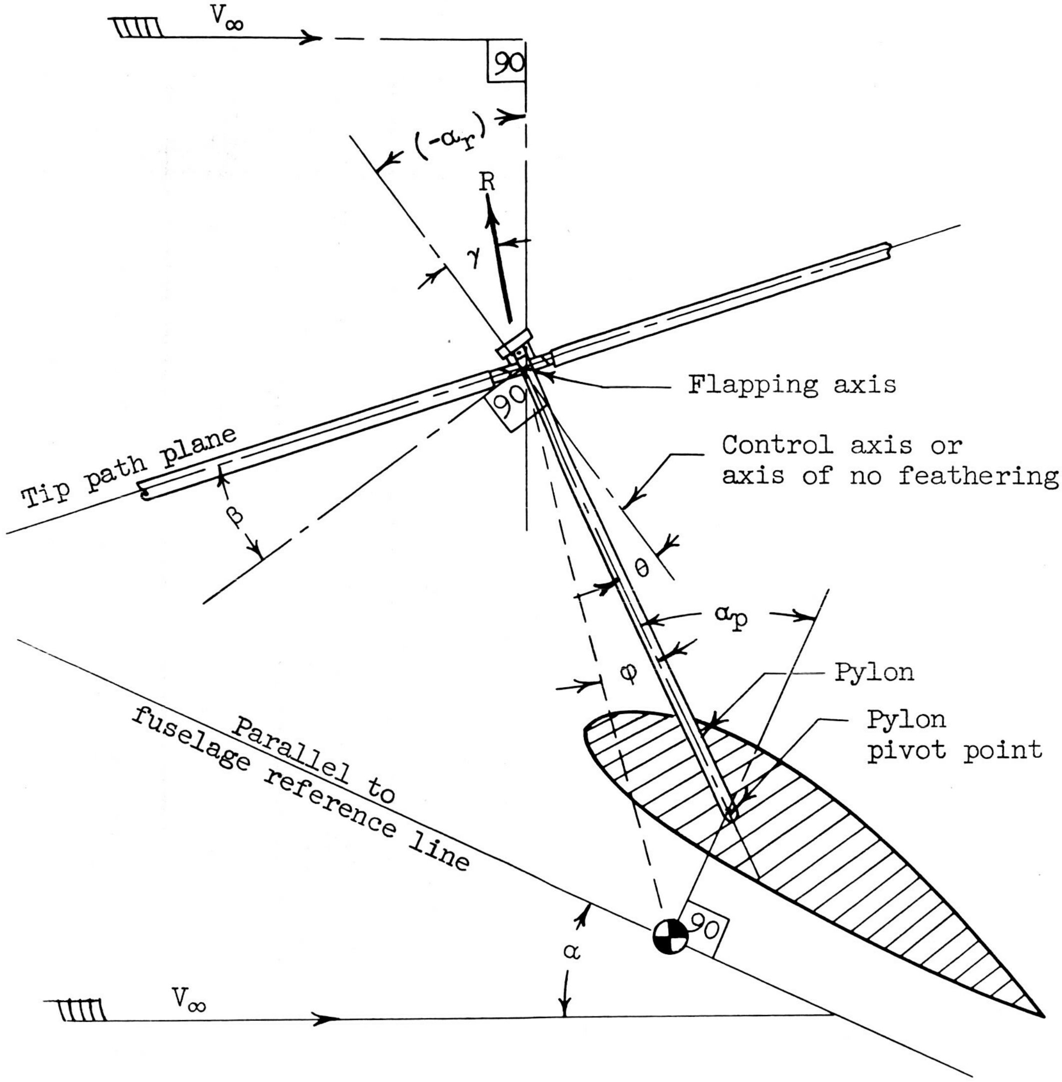

Figure 1.- Angle convention, shown in plane parallel to aircraft plane of symmetry.

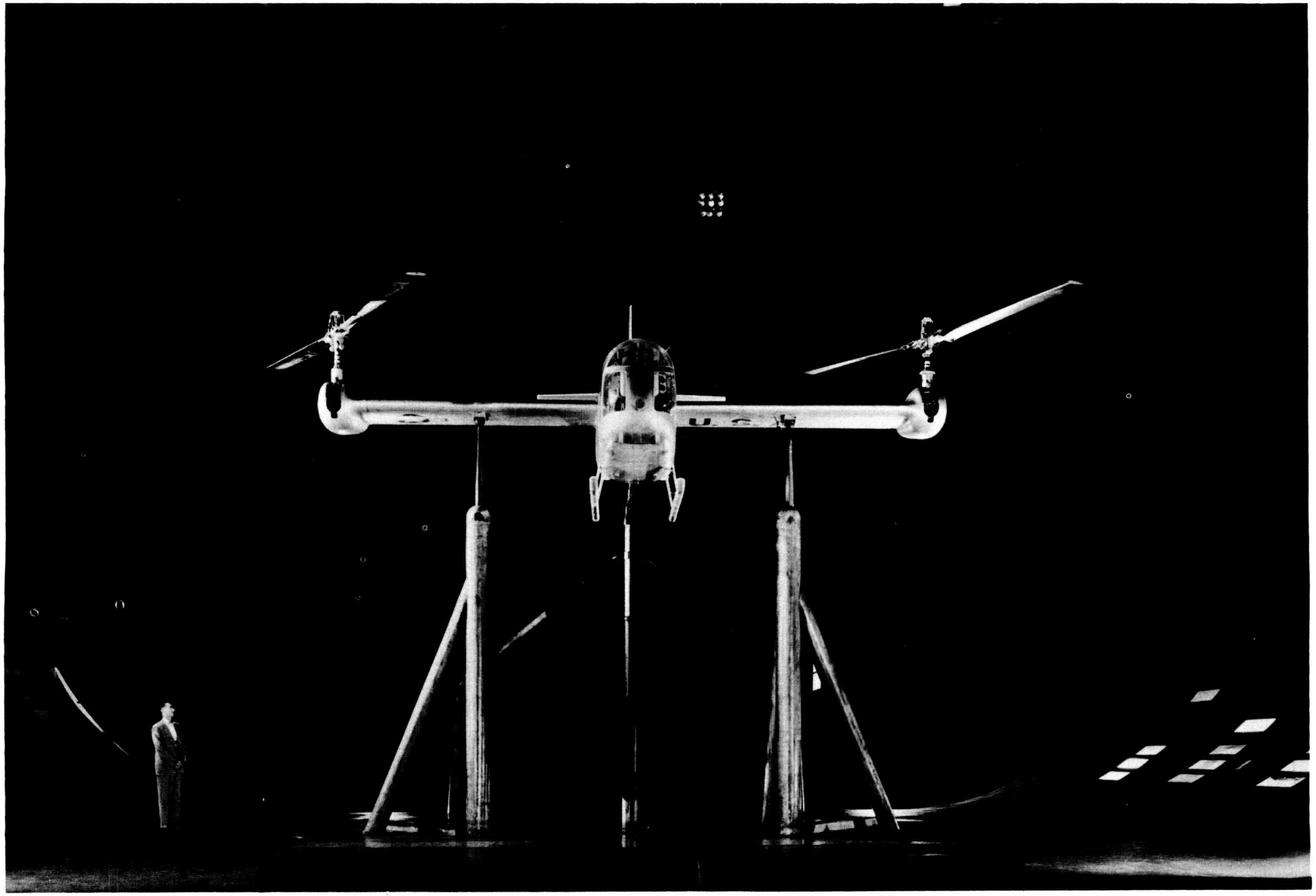

A-23165

(a) View of aircraft with short pylons and tip fairings.

Figure 2.- Photograph of the XV-3 mounted in the Ames 40- by 80-foot wind tunnel; pylons in helicopter position.

A-23002

(b) View of aircraft without tip fairings and with long pylons.

Figure 2.- Continued.

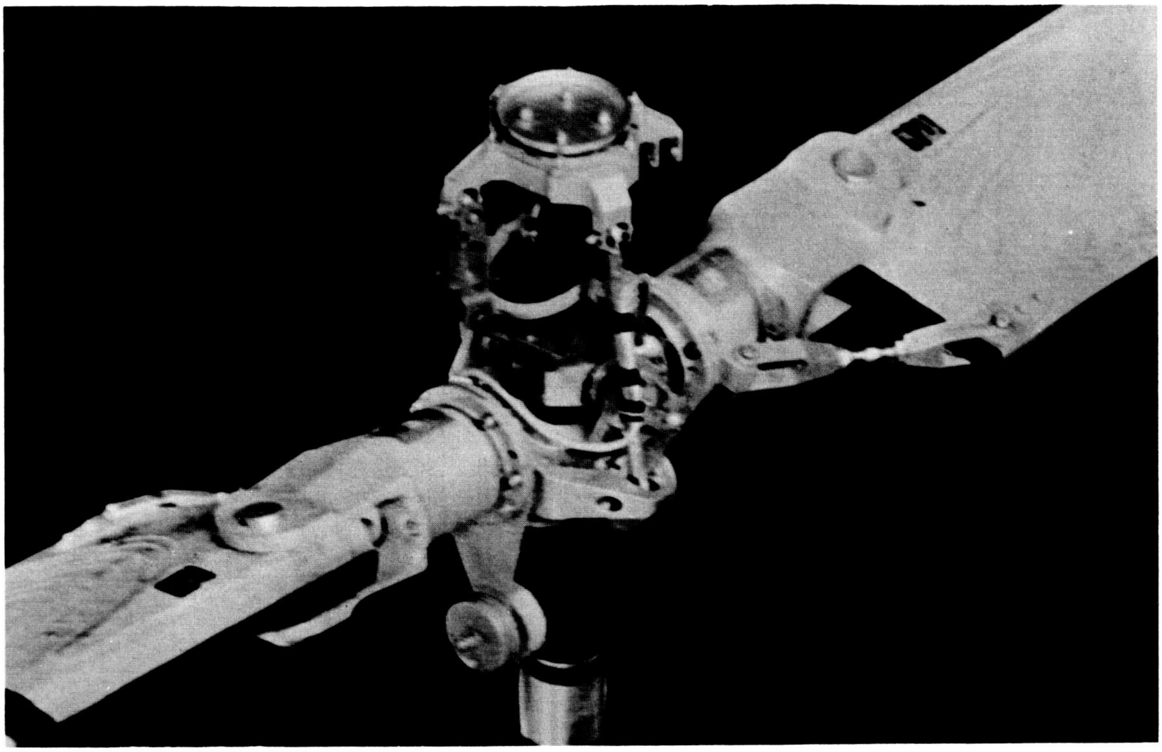

A-23002

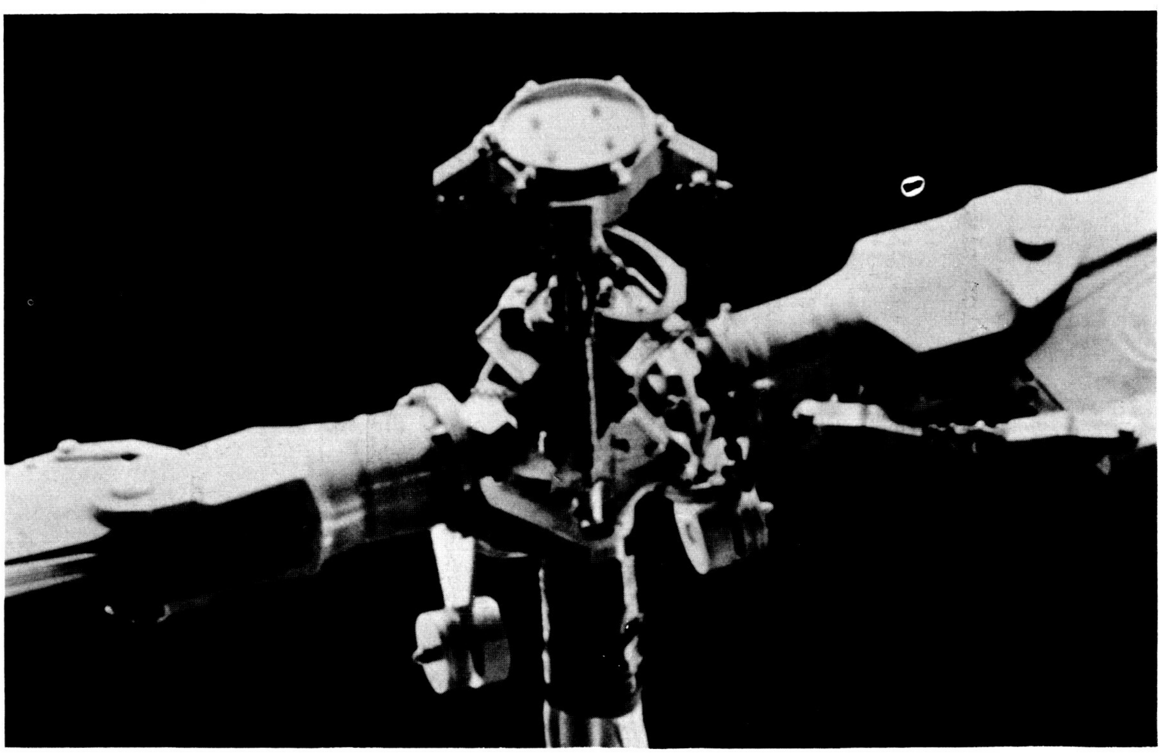

A-23003

(c) Views of rotor hub assembly.

Figure 2.- Concluded.

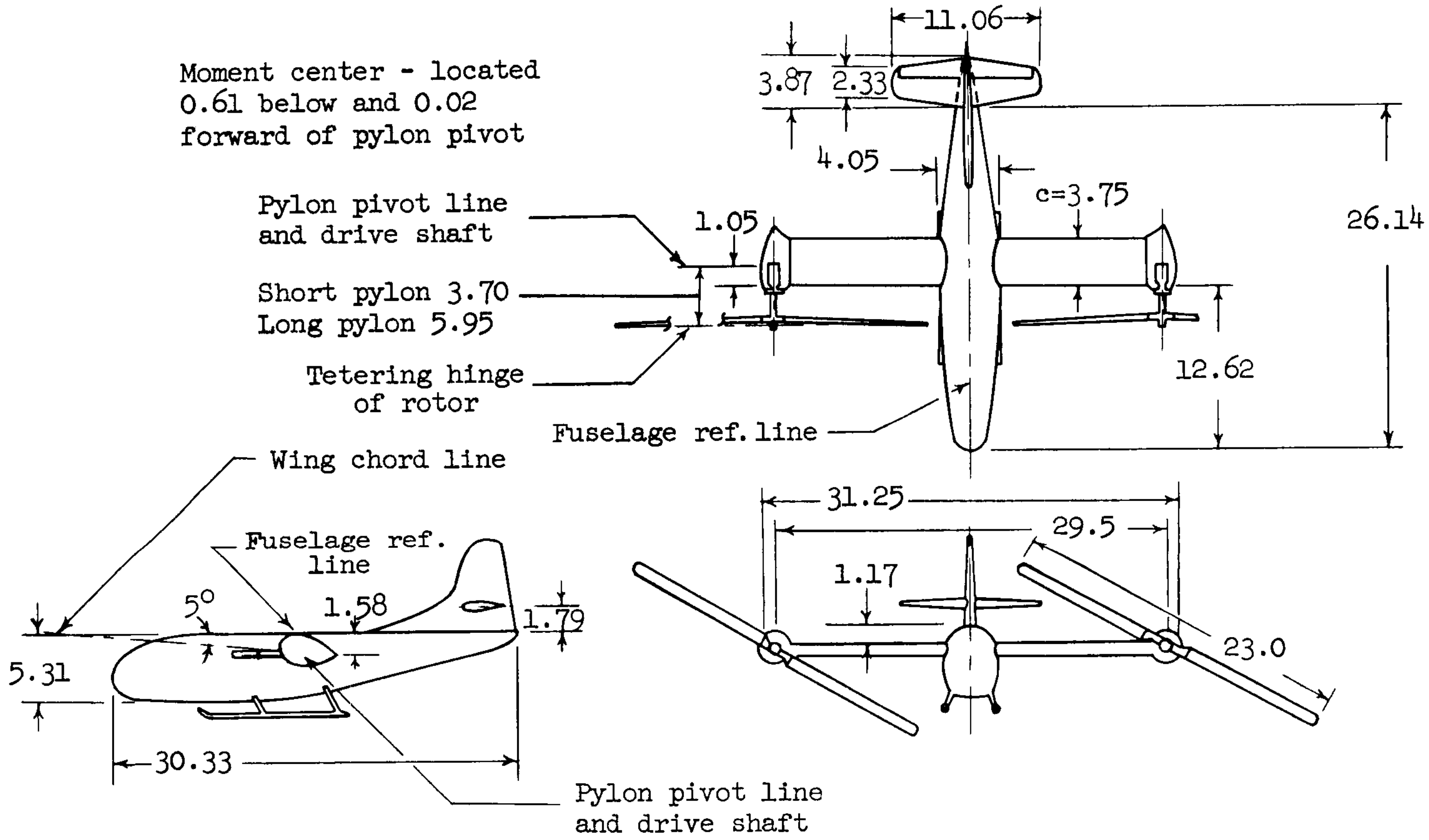

Figure 3.- Three-view drawing of the XV-3; all dimensions shown in feet.

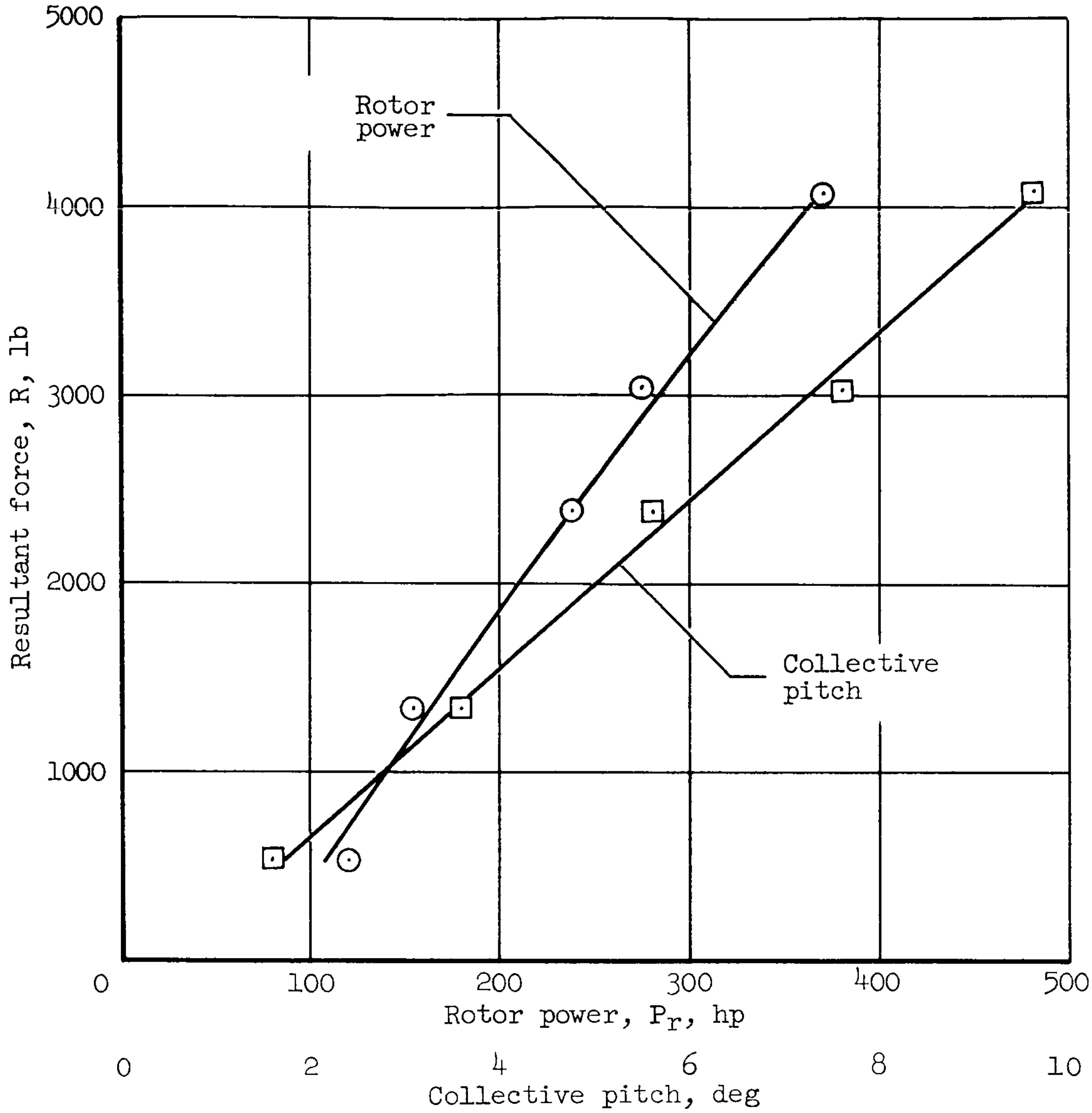

(a) Resultant force at zero airspeed; $\alpha_p = 5^\circ$; rotor diameter, 23 ft.

Figure 4.- Force characteristics near hovering conditions; overhead doors in test section open; $\alpha = 0^\circ$; rotor speed = 532 rpm.

A-165

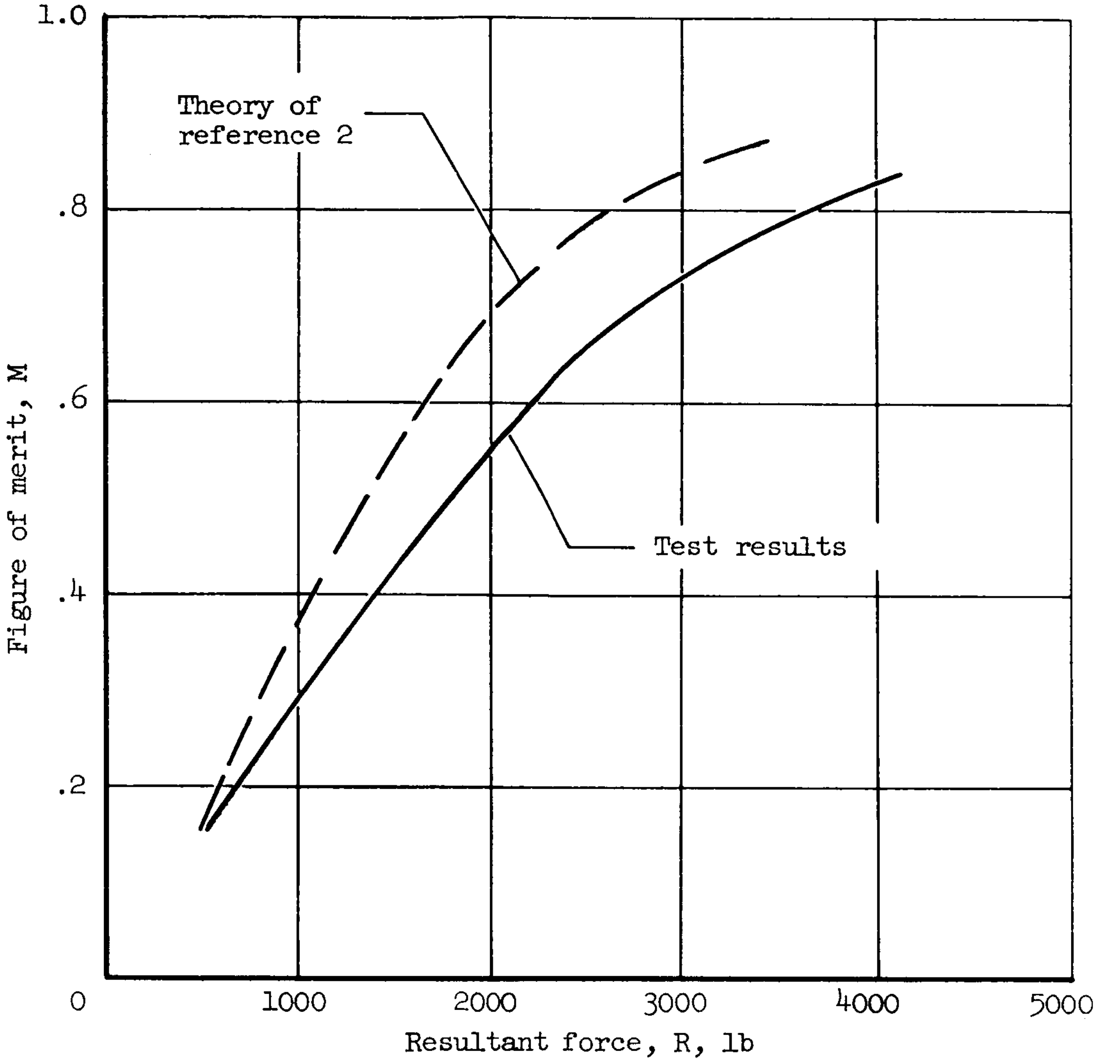

(b) Figure of merit.

Figure 4.- Concluded.

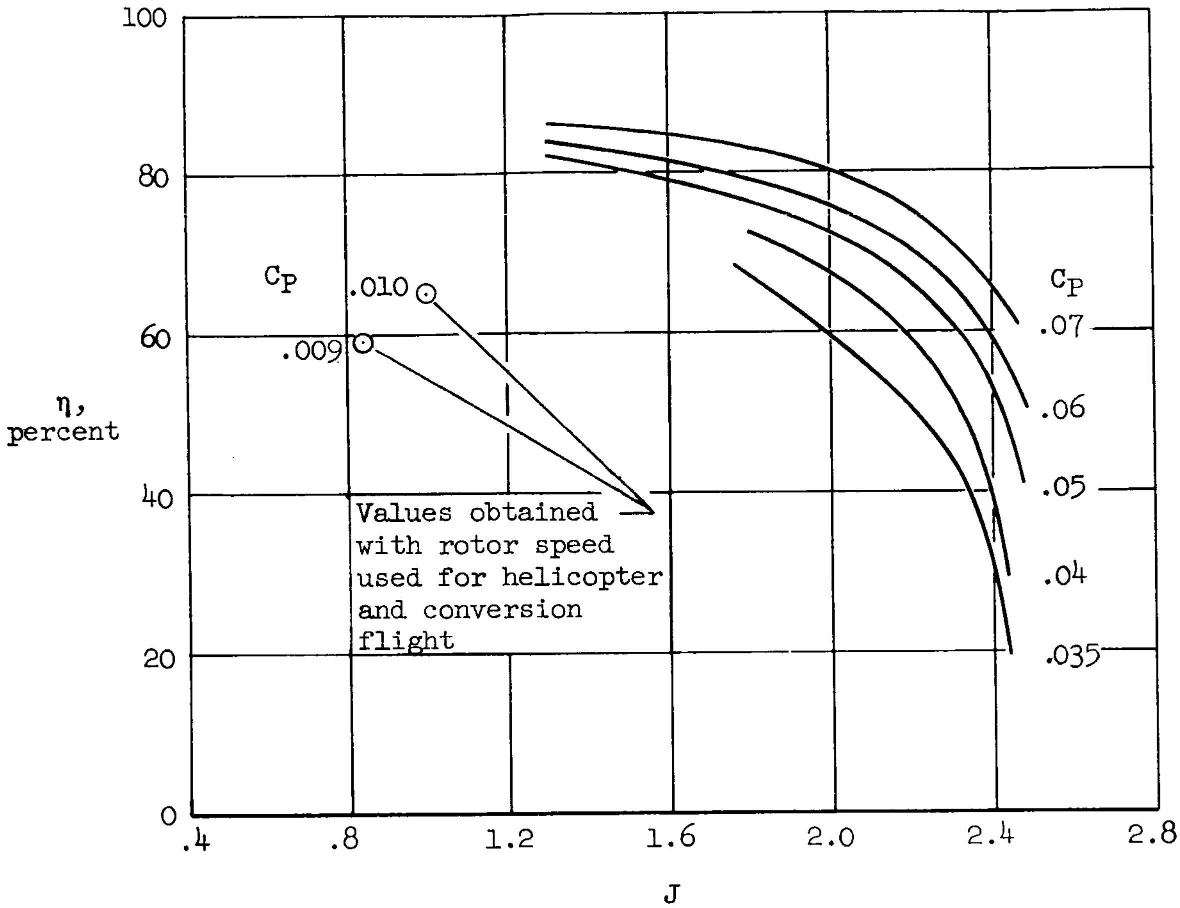

Figure 5.- Propulsive efficiency of the XV-3 rotor combination measured during the tests; $\alpha = 0^{\circ}$. Faired curves obtained with rotor speeds used for airplane flight.

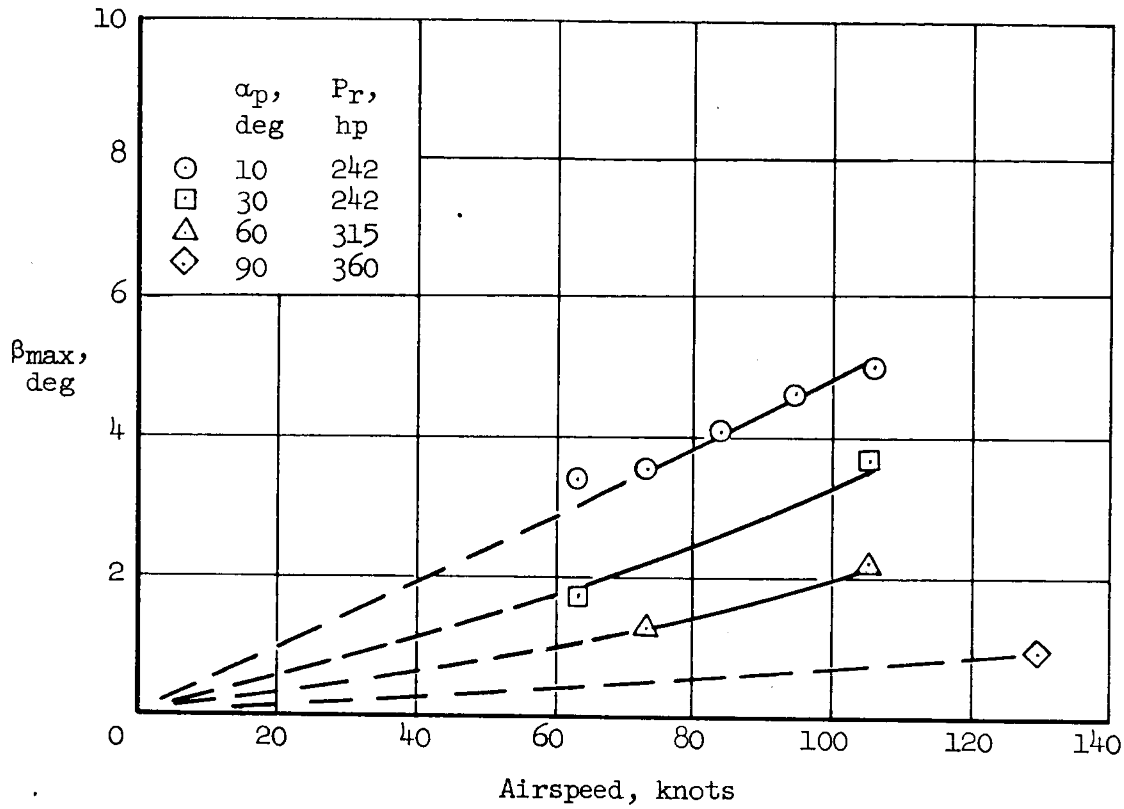

(a) Effect of pylon angle on rotor flapping for a rotor speed of 532 rpm; $\alpha = 0^{\circ}$.

Figure 6.- Results of measurements of maximum rotor flapping for the XV-3; $\theta = 0^{\circ}$.

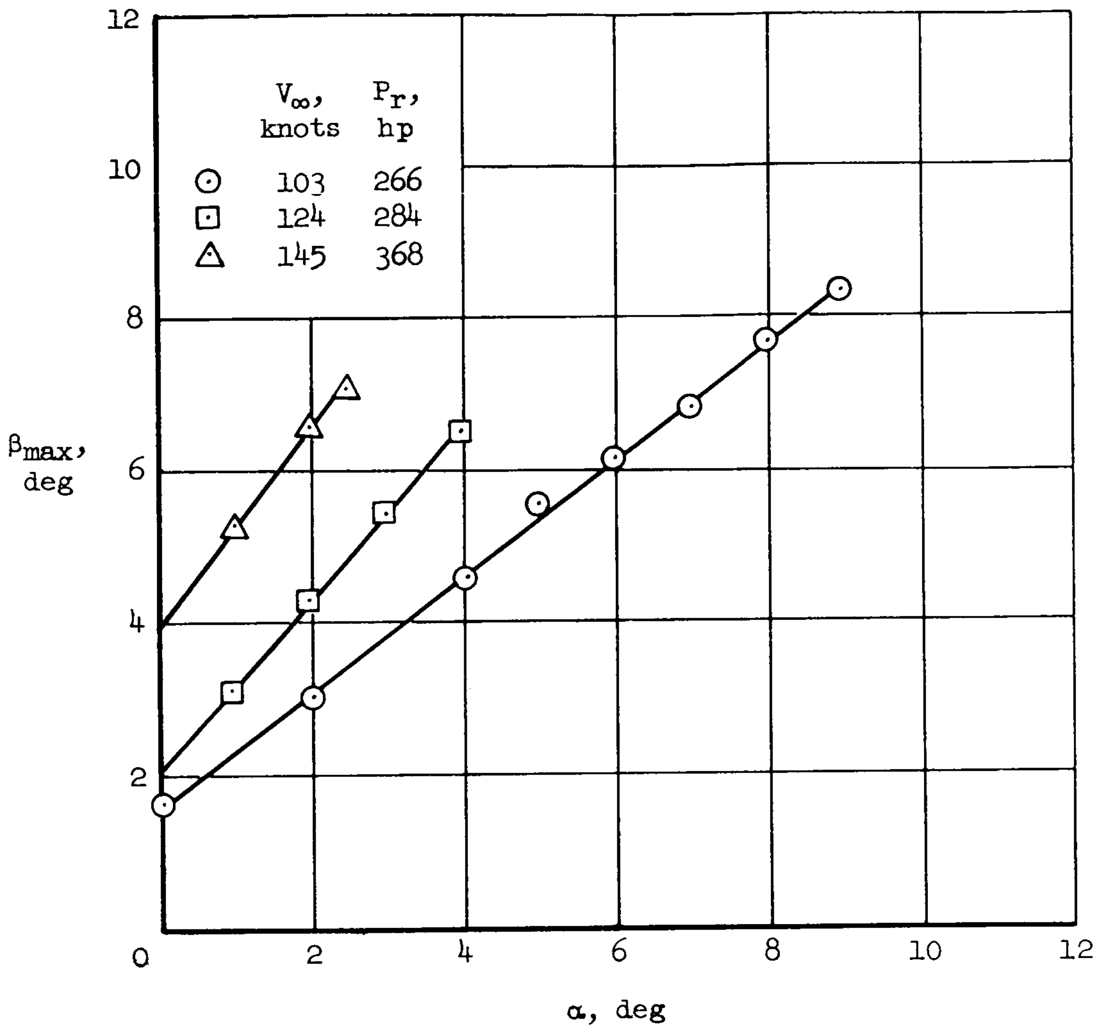

(b) Effect of airspeed on maximum flapping for the airplane configuration; $\alpha_p = 90^\circ$; rotor speed = 275 rpm.

Figure 6.- Concluded.

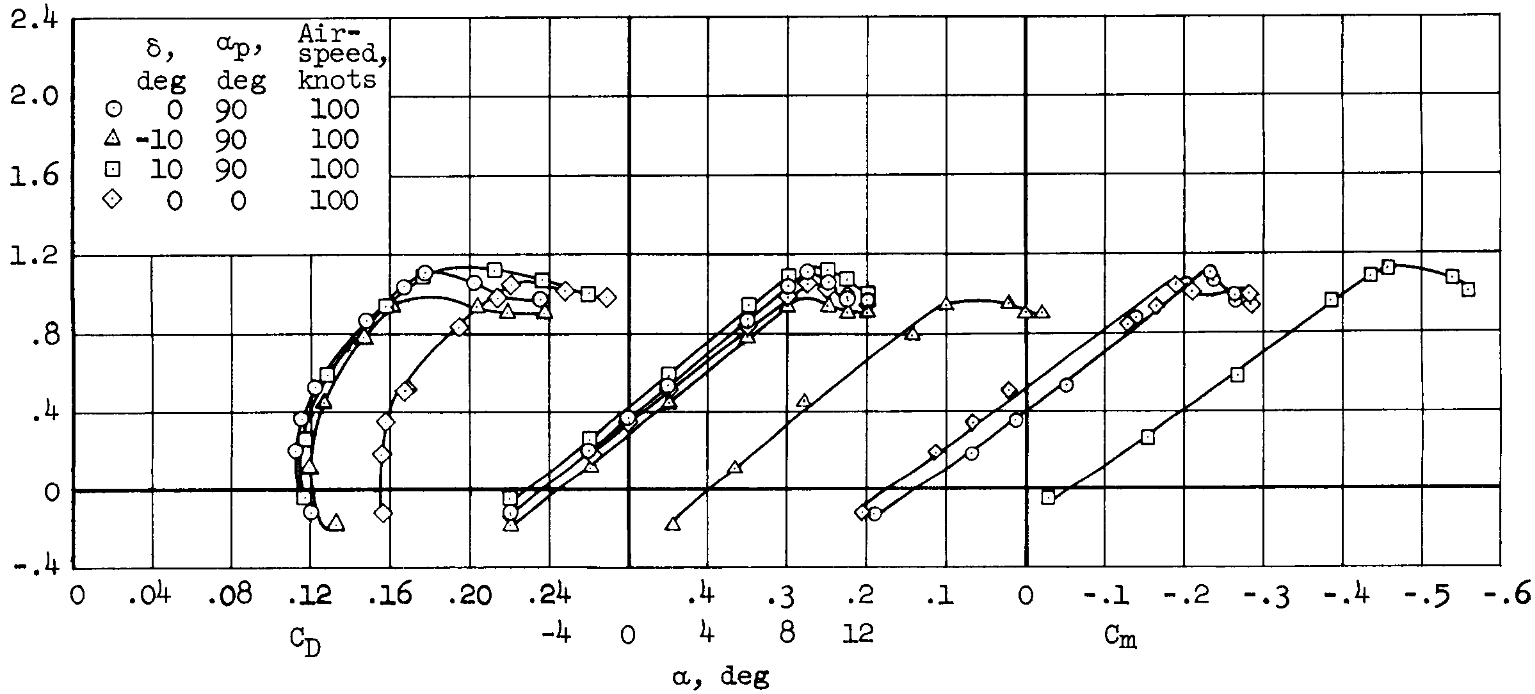

Figure 7.- Aerodynamic characteristics of the XV-3 with the rotor blades off.

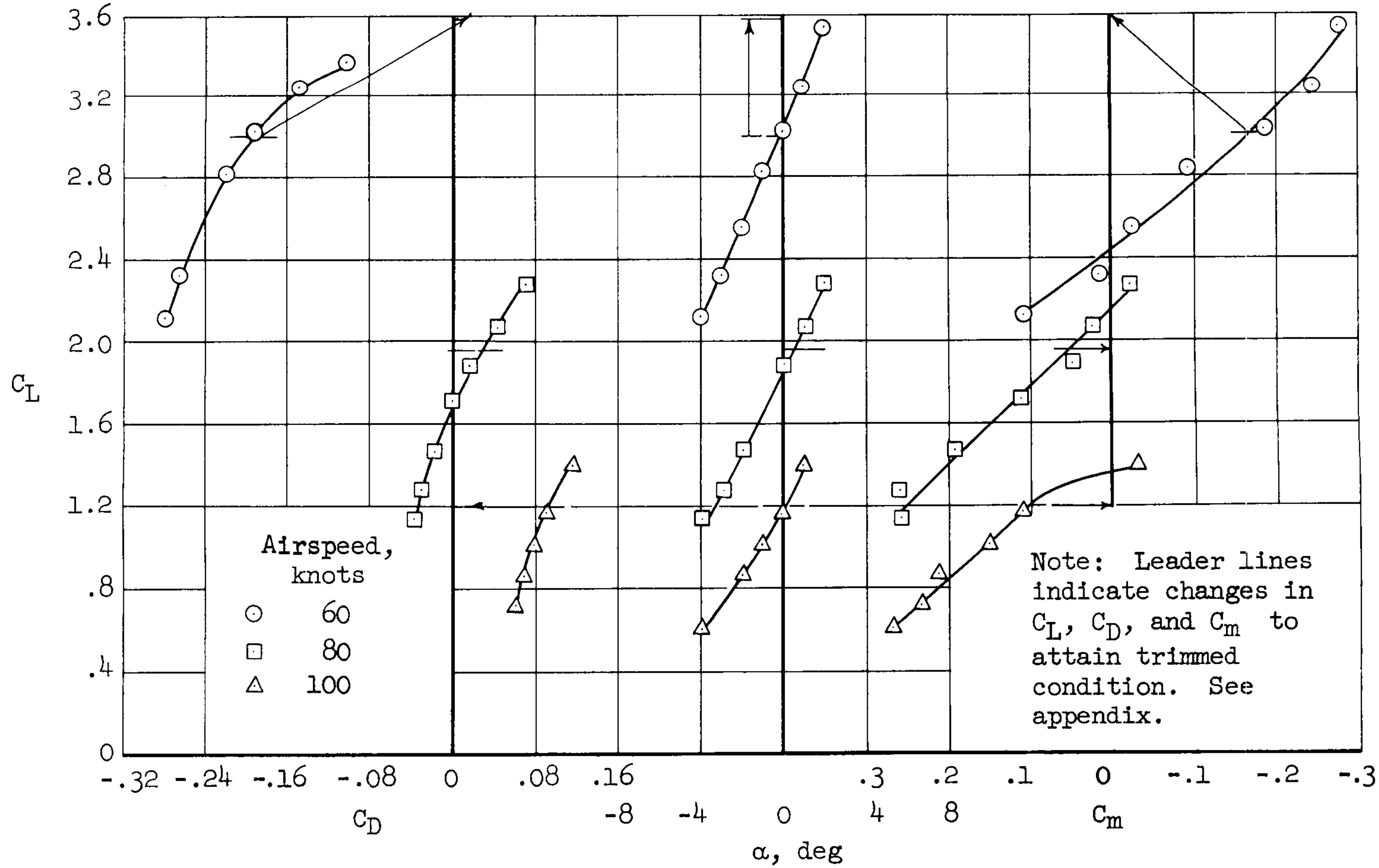

(a) $\alpha_p = 10^{\circ}$; $\theta = 0.7^{\circ}$; $\delta = -4.8^{\circ}$; $P_r = 242$ hp

Figure 8.- Aerodynamic characteristics of the XV-3; rotor speed = 532 rpm.

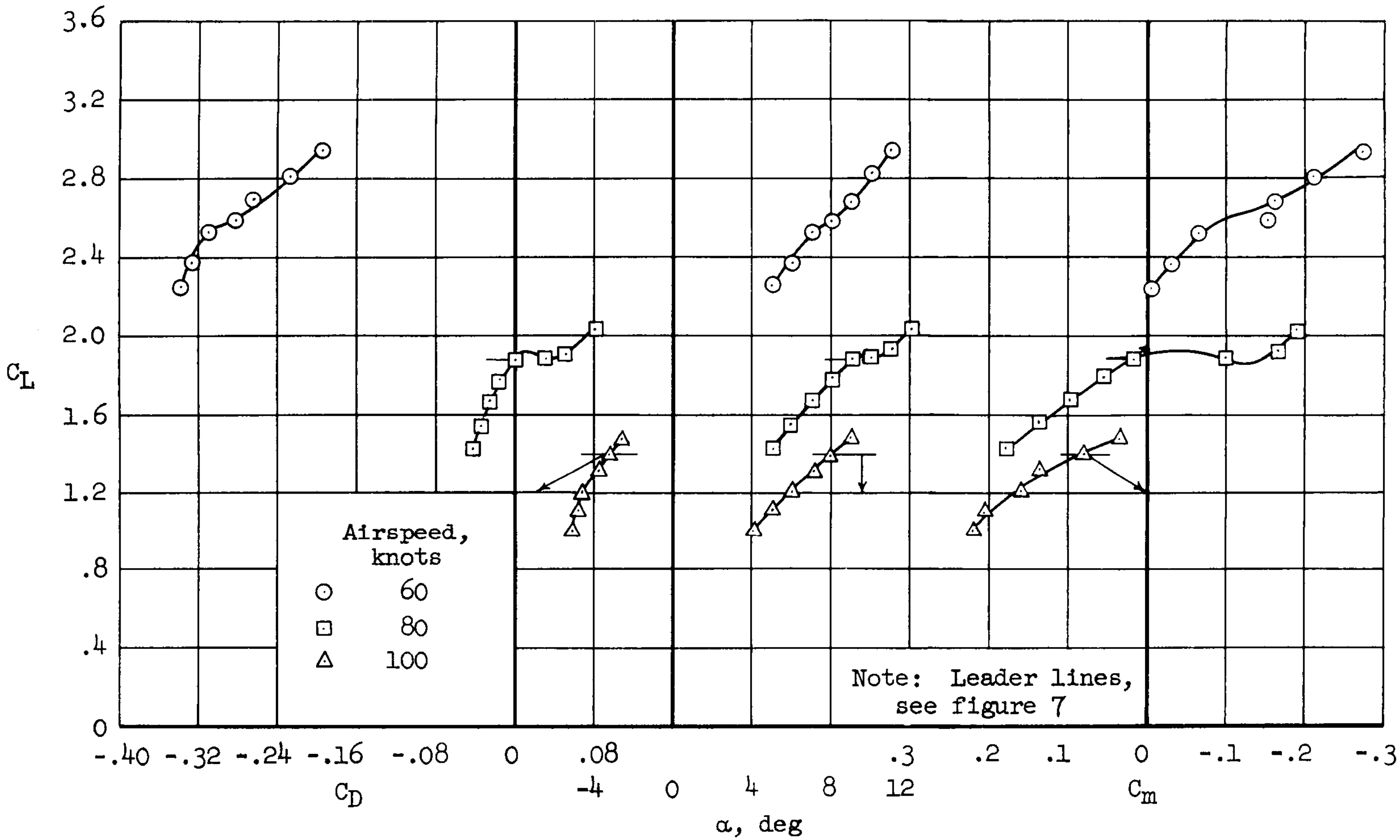

(b) $\alpha_p = 30^\circ$; $\theta = 0^\circ$; $\delta = -9^\circ$; $P_r = 242$ hp

Figure 8.- Continued.

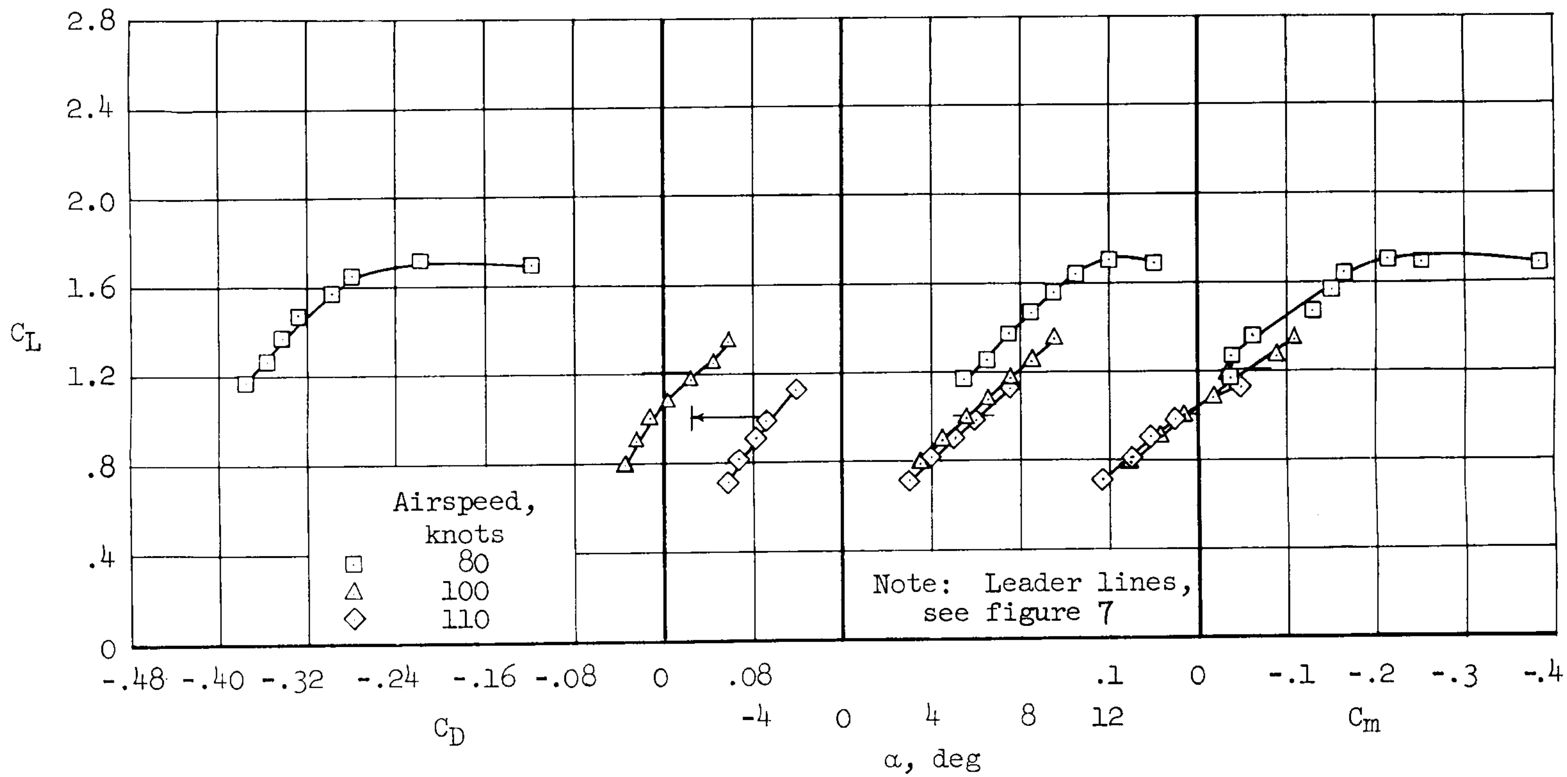

(c) $\alpha_p = 60^\circ$; $\theta = 0.3^\circ$; $\delta = -4^\circ$; $P_r = 311$ hp

Figure 8.- Continued.

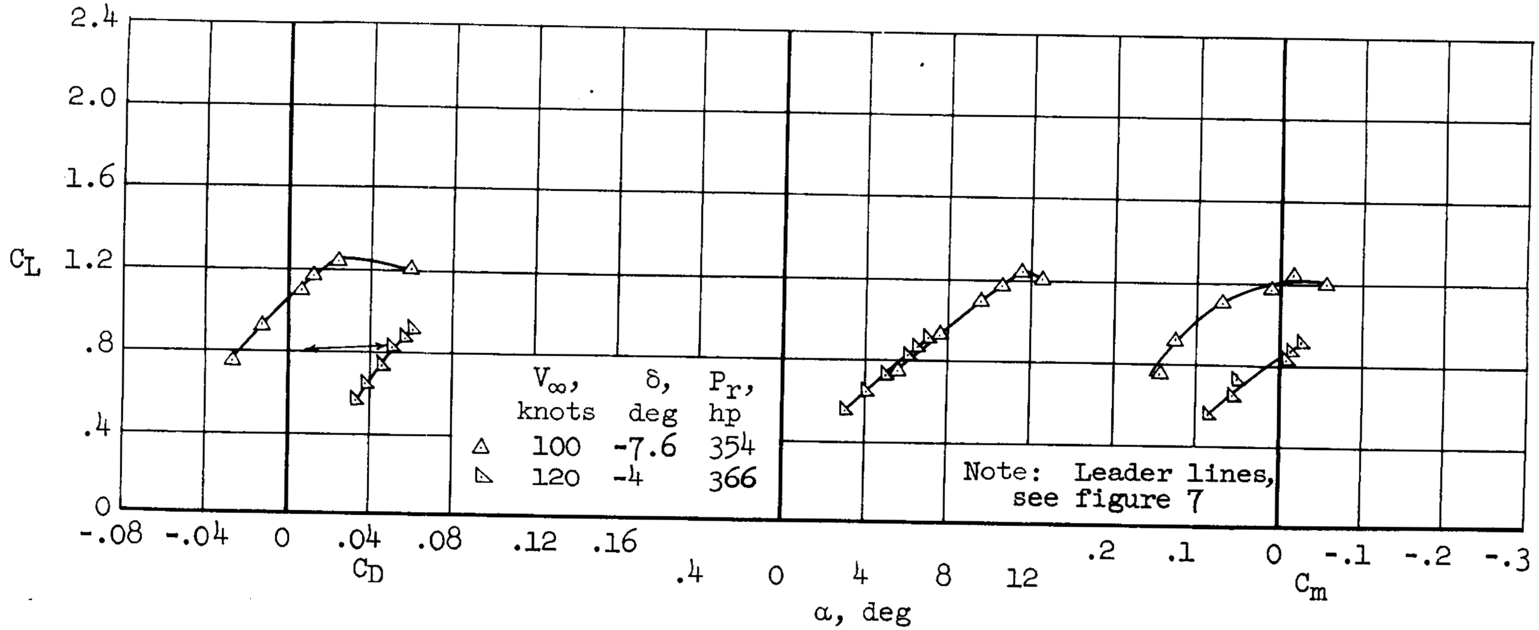

(d) $\alpha_p = 90^{\circ}$

Figure 8.- Concluded.

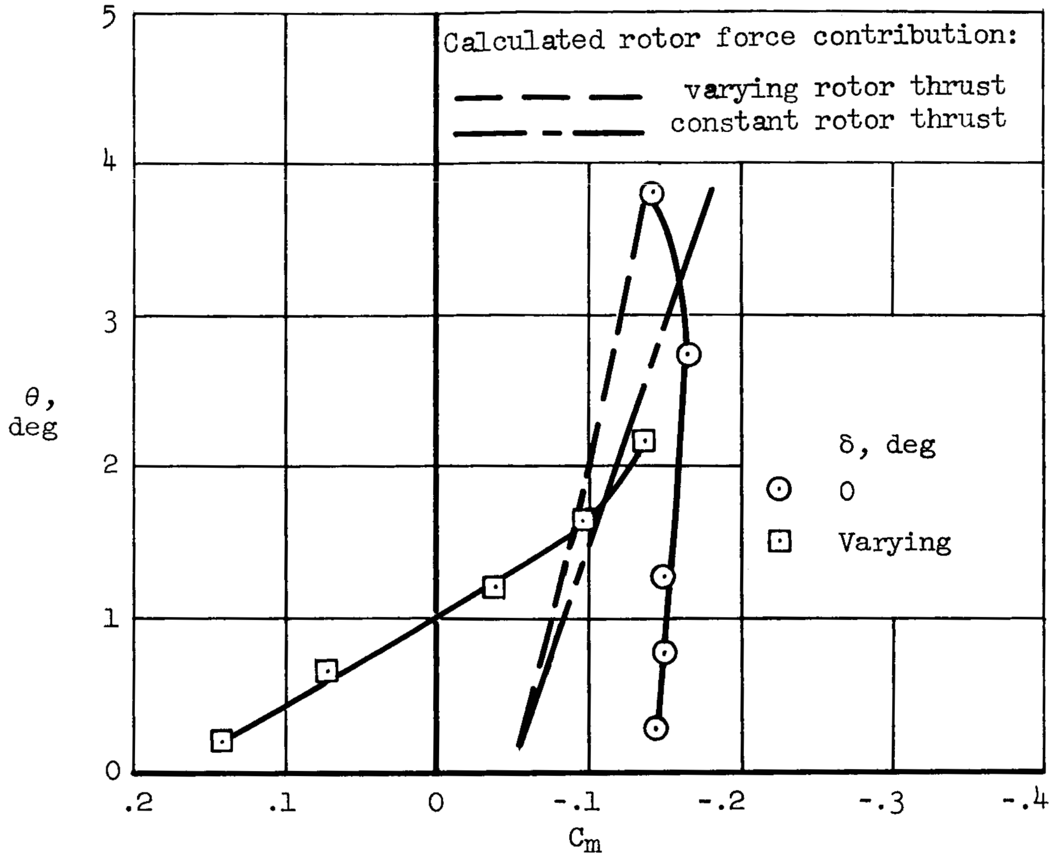

Figure 9.- Longitudinal control at $\alpha_p = 10^\circ$ with and without the use of the elevator; rotor driven with 242 hp at 532 rpm; $\alpha = 0^\circ$; $V_\infty = 80$ knots.

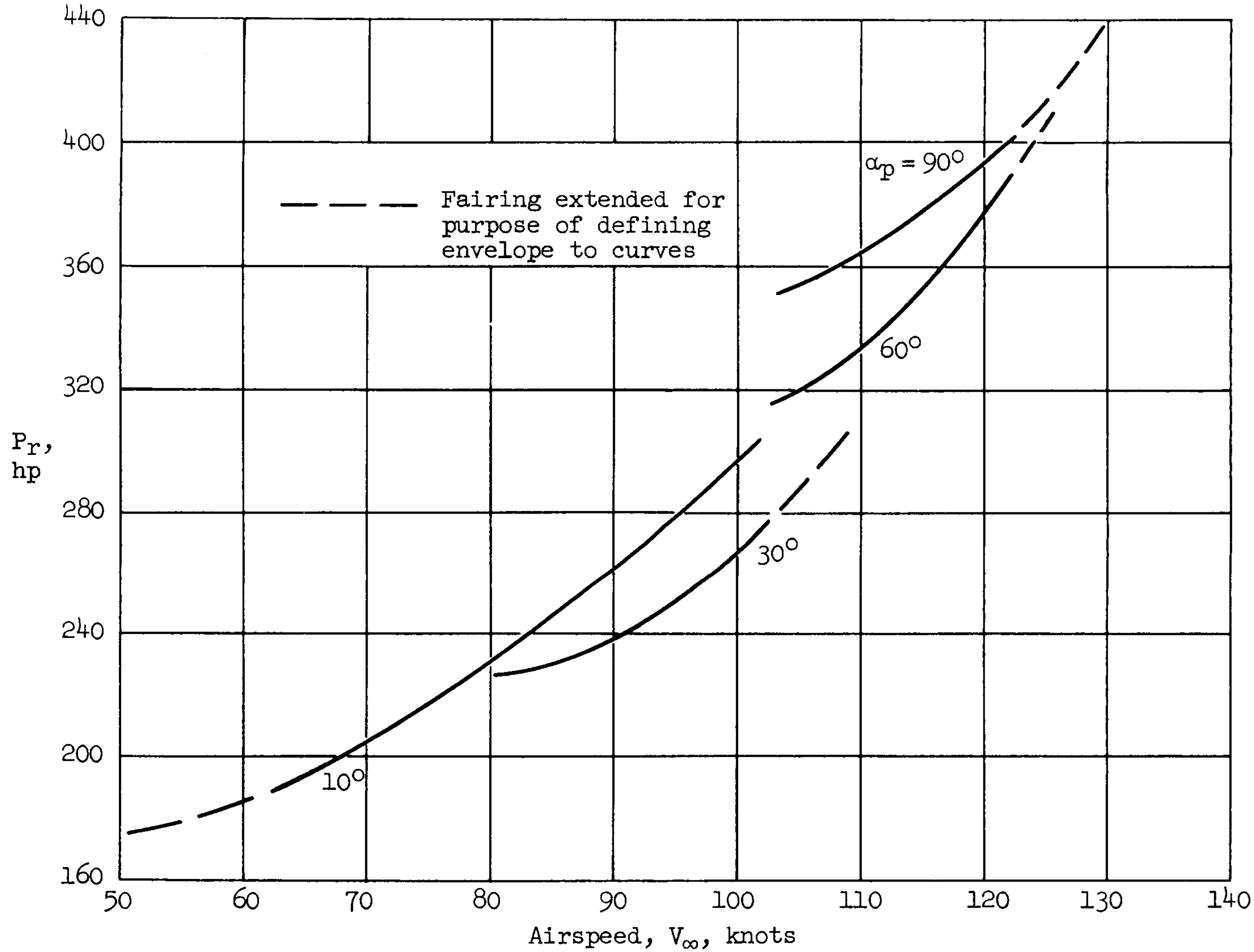

(a) Rotor horsepower, P_r.

Figure 10.- The variation with airspeed of rotor horsepower, elevator setting, and angle of attack for trimmed level flight at 4700 pounds lift; rotor speed = 532 rpm.

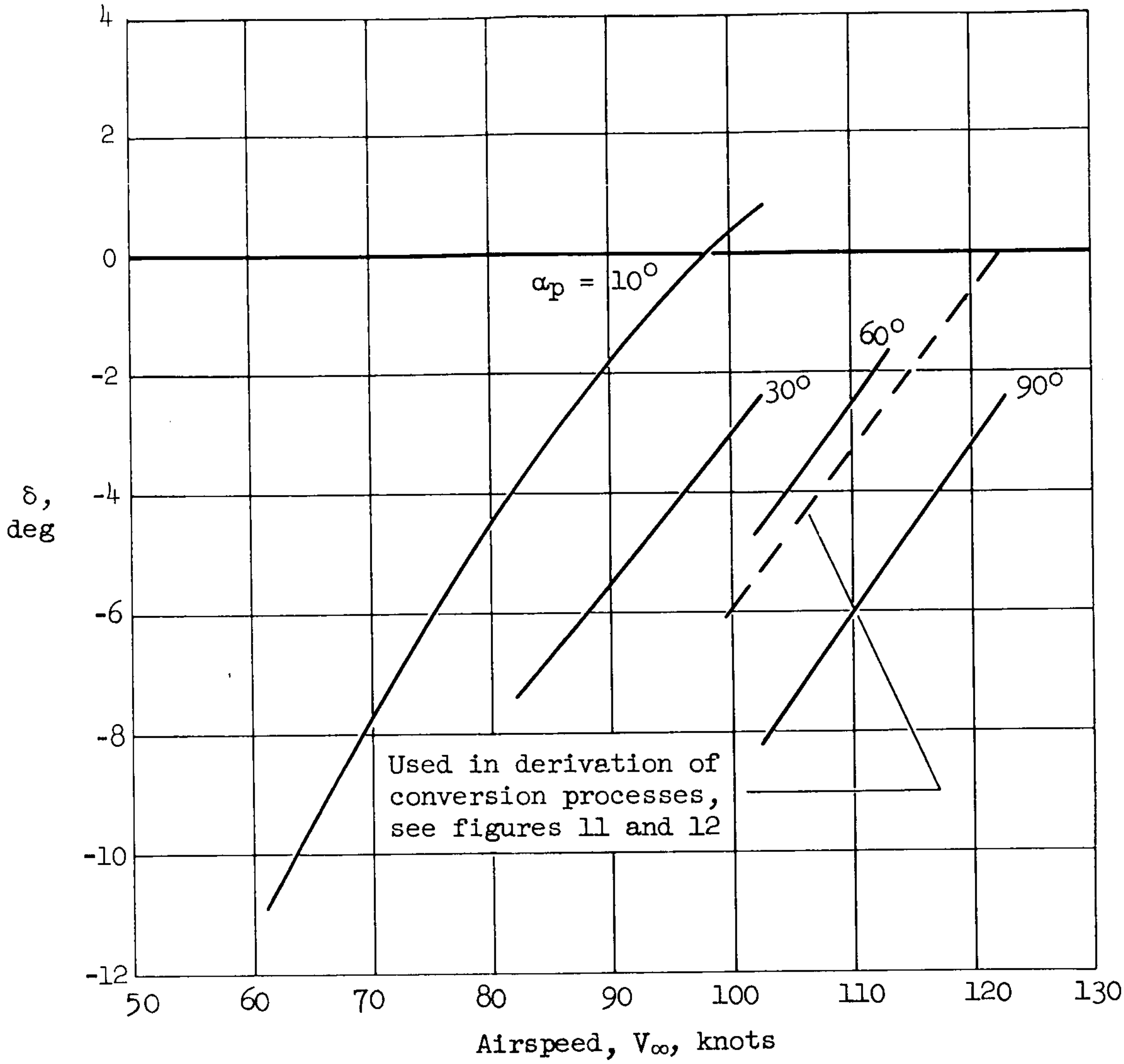

(b) Elevator setting, δ.

Figure 10.- Continued.

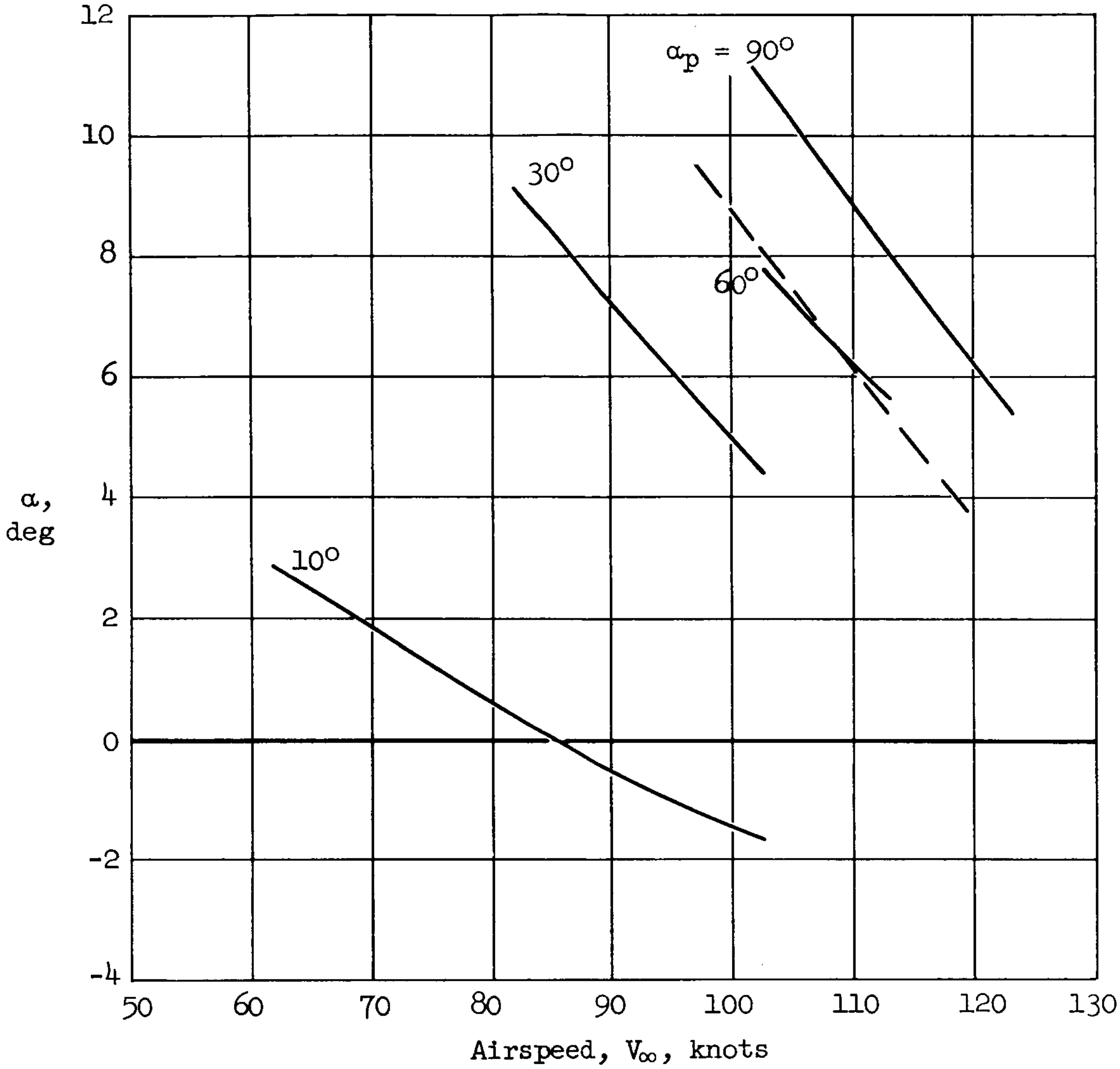

(c) Fuselage angle of attack, α.

Figure 10.- Concluded.

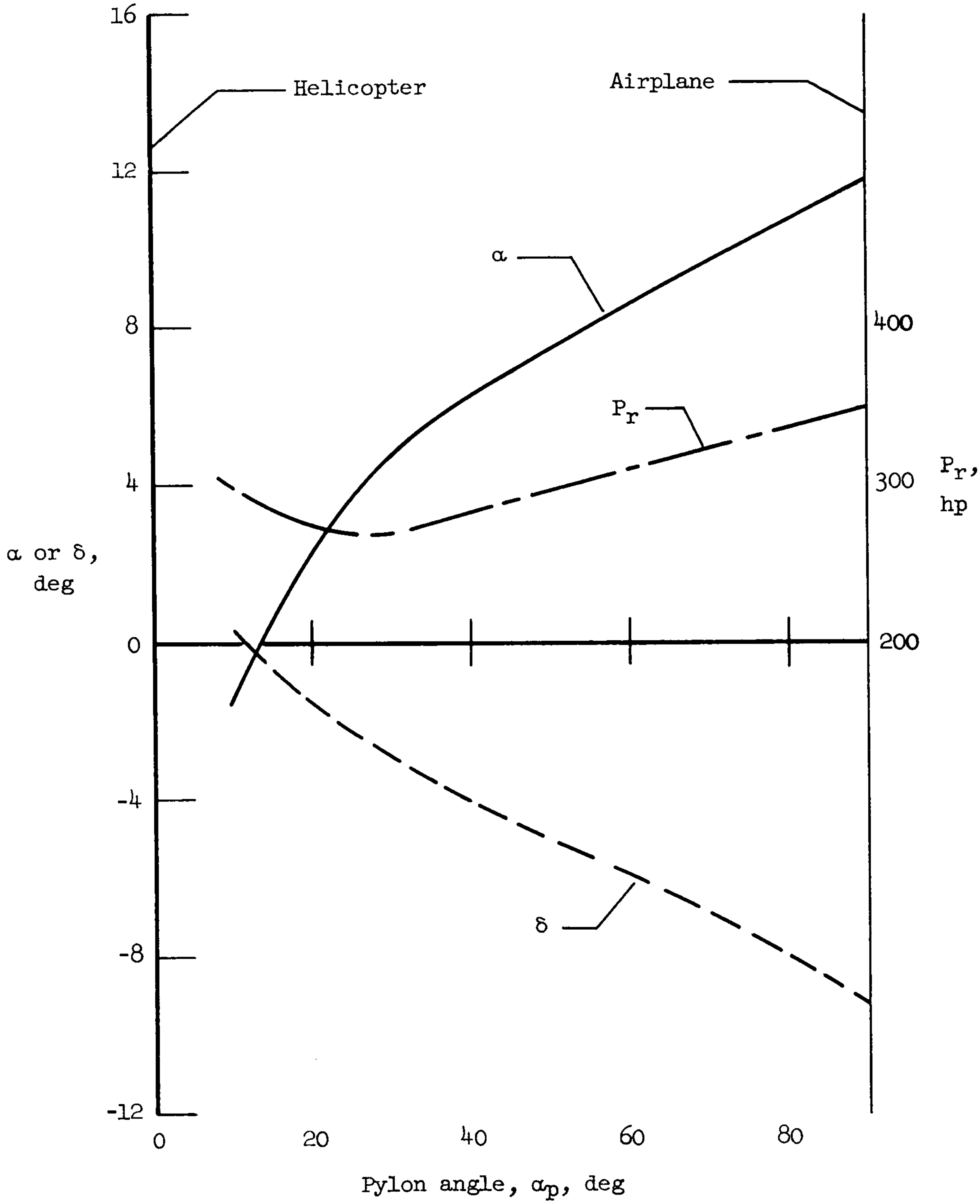

Figure 11.- Angle of attack, rotor horsepower, and elevator angle of the XV-3 required for level flight conversion at a constant airspeed of 100 knots.

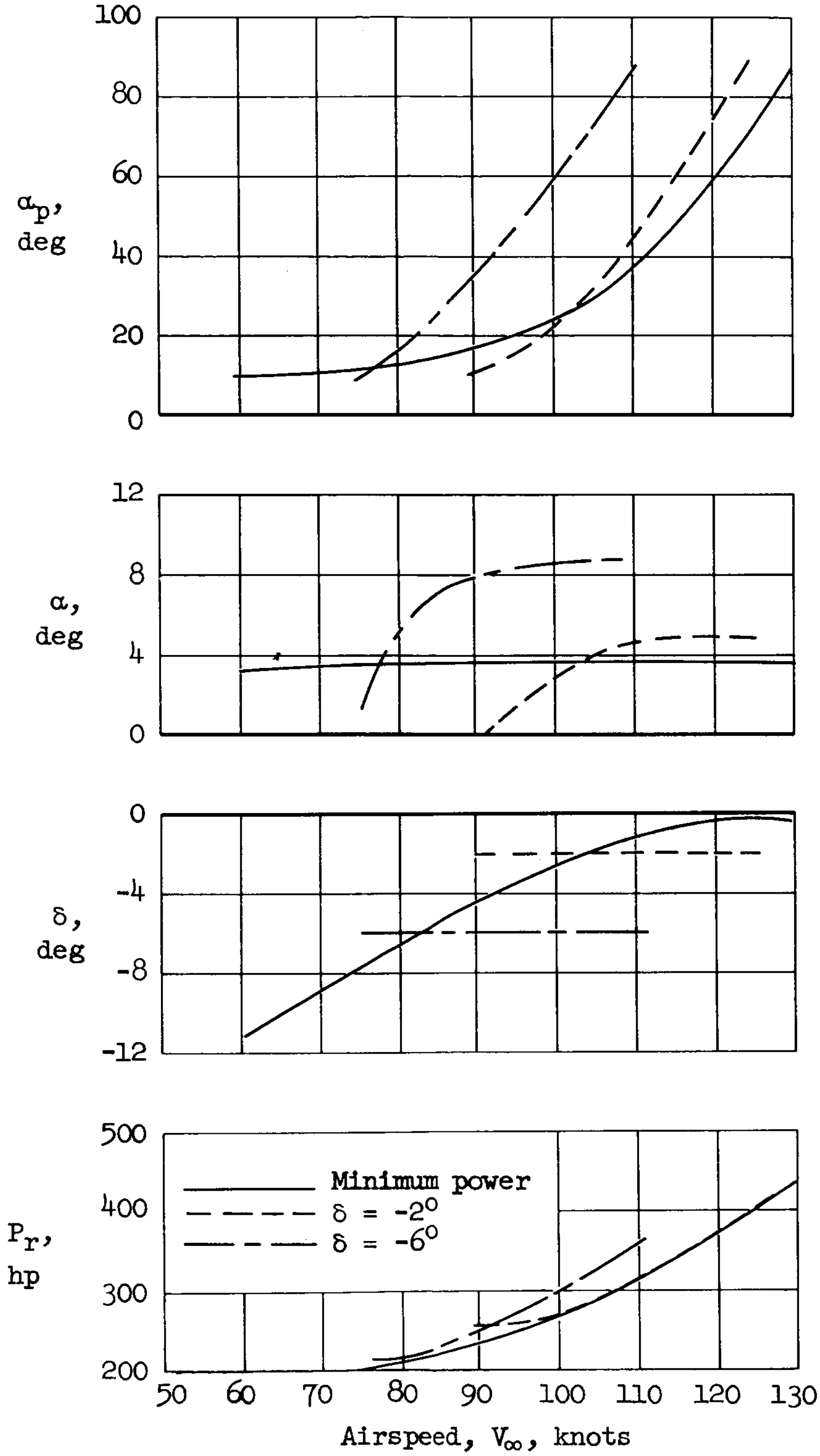

Figure 12.- Three conversion processes at varying airspeed for the XV-3 in level flight.